UDC 621.3 https://doi.org/10.20998/2074-272X.2025.3.11

B. Yahiaoui, A. Messaoudene, A. Melahi, A. Rahmani, B. Bendahmane, L. Dascalescu

Efficiency of neutralization of electric charges on the surface of dielectric nonwoven fabric of two dual and triode electrode systems

Introduction. *The accumulation of electrostatic charges are exploited in various technological and industrial applications, but they can also pose significant challenges, especially due to the accumulation in inappropriate locations that can reach dangerous levels.* ***Problem***. *The static charges are often considered annoying and constitute one of the main sources of hazards. Thus, their neutralization is more than necessary.* ***The objective*** *of this work is to improve the neutralization rate with equipment that can be easily integrated in the production lines.* ***Novelty***. *The paper reports a comparative study of the neutralization efficiency of two electrode systems, dual and triode, with different high alternating voltages at the industrial frequency of 50 Hz. The use of the industrial frequency of 50 Hz reduces the elements of the neutralization equipment. By connecting the grid to ground, we aim to impose a zero potential on the surface of the initially charged polypropylene fibrous dielectric and to determine the variation of the neutralization rate as a function of the discharge intensity (voltage amplitude).* ***Methodology.*** *The samples were charged during 10 s using a triode-type corona electrode configuration supplied by negative or positive DC high voltage. After 300 s of the charging process. The neutralization was performed during 4 s, using the dual or the triode systems powered by sinusoidal high voltage. Neutralization efficiency is achieved by non-contact sampling of surface potential profiles before and after neutralization.* ***The results*** *show that neutralization efficiency is proportionate to the discharge current intensity. The neutralization using the triode system is more efficient. The results show the possibility of imposing a desired potential on the charged or uncharged dielectric surface by acting on the potential of the metallic grid and the discharge intensity of the triode system.* ***Practical value.*** *The results demonstrate the proportionality of the neutralization efficiency with the discharge intensity for the triode system. Therefore, an adjustment of the voltage amplitude is necessary in order to optimize its efficiency for the dual system.* References 30, figures 7.
Key words: **surface potential, corona discharge, charge neutralization, fibrous electrets, triode system.**

Вступ. *Накопичення електростатичних зарядів використовуються в різних технологічних та промислових застосуваннях, але вони також можуть становити значні проблеми, особливо через накопичення в невідповідних місцях, що може досягати небезпечних рівнів.* ***Проблема*** *полягає в тому, що статичні заряди часто вважаються неприємними і є однією з основних причин небезпек. Тому їх нейтралізація є більш ніж необхідною.* ***Метою*** *роботи є покращення рівня нейтралізації за допомогою обладнання, яке можна легко інтегрувати в виробничі лінії.* ***Новизна.*** *У статті представлено порівняльне дослідження ефективності нейтралізації двох електродних систем:діодної та тріодної, при різних високих змінних напругах на промисловій частоті 50 Гц. Використання промислової частоти 50 Гц зменшує кількість елементів нейтралізаційного обладнання. Підключення сітки до землі дозволяє нав'язати нульовий потенціал на поверхні початково зарядженого поліпропіленового волокнистого діелектрика та визначити зміну рівня нейтралізації залежно від інтенсивності розряду (амплітуди напруги).* ***Методологія.*** *Зразки заряджали протягом 10 с за допомогою електродної конфігурації типу тріода, живленої негативною або позитивною постійною високою напругою. Після 300 с заряджання, нейтралізація проводилась протягом 4 с за допомогою подвійних або тріодних систем, живлених синусоїдальною високою напругою. Ефективність нейтралізації визначалась шляхом безконтактного зняття профілів поверхневого потенціалу до та після нейтралізації.* ***Результати*** *показали, що ефективність нейтралізації пропорційна інтенсивності розрядного струму. Нейтралізація за допомогою тріодної системи є більш ефективною. Результати показують можливість нав'язати бажаний потенціал на зарядженій або незарядженій діелектричній поверхні, впливаючи на потенціал металевої сітки та інтенсивність розряду тріодної системи.* ***Практична цінність.*** *Результати демонструють пропорційність ефективності нейтралізації до інтенсивності розряду для тріодної системи. Тому коригування амплітуди напруги є необхідним для оптимізації її ефективності для подвійної системи.* Бібл. 30, рис. 7.
Ключові слова: **поверхневий потенціал, коронний розряд, нейтралізація зарядів, волокнисті електрети, тріодна система.**

Introduction. The use of static electricity extends to various technological and industrial fields [1, 2], including electrostatic painting, the removal of dust from waste gases [3, 4], the separation of granular materials [5], and the creation of electrets transducers [2]. Fibrous polymers such as polypropylene, polycarbonate, polyurethane and polyethylene are often used in electrostatic filters for their ability to retain electrical charges for a long time [6]. However, the charge accumulated on these materials due to different physical phenomena of charging generally by triboelectric effect are inherent to the manufacturing process and can be harmful either to the operator or to sensitive electronic equipment and components. In the electronics manufacturing industry, the main hazard is the static charge accumulated on the manipulator's suits [7]. Indeed, electrostatic discharges can interrupt the contacts and the connection of increasingly miniaturized electronic components. Electrostatic discharges cause considerable damage in different industries, oil, electronics, textiles, etc. On the other hand, static electricity is subject to several studies aiming to improve some processes [2, 5], to develop new applications and to limit their negative effects [7, 8].

Corona discharge effects are exploited in various industrial applications [9], ranging from surface and material treatment, water treatment and air purification [10, 11] to electrostatic charge neutralization [12] and electrical network diagnostics [13]. Due to various applications, corona discharge is the subject of several researches [14–16]. For open, delicate or sensitive surfaces, the most effective method of controlling static electricity is active neutralization using a corona discharge, because this method does not require direct contact with the surface to be neutralized. Compared with other neutralization methods, corona discharge can be more energy-efficient [17–19].

The corona electrode is energized by different amplitudes of high voltages (HV) at high frequencies [8]. Several studies have been carried out on the active neutralization of the charge present on the surface of films [20–22], granules and non-woven fibrous materials [23]. In previous studies, the authors used the same method to evaluate the effect of wave forms of the HV at different

frequencies on the neutralization efficiency using dual electrode system [24]. Also, they evaluated the effect of charging time, neutralization time, the frequency and the amplitude of AC HV on the neutralization efficiency [23]. Using the triode system, the authors were interested in the effects of successive neutralizations with increasing discharge intensities and also the effects of the neutralization modes (fixed or scanning) on the neutralization efficiency [25]. Despite the high degree of neutralization obtained in previous work, the complete neutralization has not been achieved yet.

The aim of this work is to improve the neutralization efficiency and to evaluate the effect of the voltage level at industrial frequency (50 Hz) as well as the effect of the polarity of the deposited charge on the neutralization efficiency. We also aim to compare the neutralization efficiency of two electrode systems, dual and triode, under the same ambient conditions.

The use of the industrial frequency of 50 Hz allows to directly using the output voltages of the autotransformer (without the function generator and the amplifier). Polypropylene samples are charged by negative or positive corona discharge using a triode electrode system. After the surface potential decay becomes almost zero [26, 27], the samples are subjected to an AC corona discharge generated by the dual electrode system in the first part of the tests and by the triode system with the grid connected directly to ground for the second part of the tests. During neutralization, both electrode systems are powered by high sinusoidal voltages at industrial frequency (50 Hz). This work aims to improve the neutralization efficiency with a simple device that is easy to incorporate into the production chain.

Materials and methods. The experiments were performed at ambient air temperature (18 °C to 23.5 °C) and relative humidity (50 % to 61 %). The samples used are 120×9 mm (Fig. 1,*e*), cut from the same nonwoven sheet of polypropylene. The electric charging of the samples was performed using a triode electrode system (Fig. 1,*a*,*b*) [28, 29], composed of a HV wire-type dual electrode [24], facing a grounded plate electrode (aluminum, 165×115 mm), and a grid electrode. The HV electrode consists in a tungsten wire (diameter 0.2 mm) suspended by a metallic cylinder (diameter 26 mm) at 34 mm distance from the axis.

The wire and the cylinder were energized from the same adjustable HV supply, 100 kV, 3 mA (model SL300 Spellman) as shown in Fig. 1,*a*. The distances between the wire and the grid and between the grid and the surface of the plate electrode were 15 mm.

The metallic grid (Fig. 1,*d*) is connected to the ground through a series of calibrated resistors of an equivalent resistance R. In this way, for a current intensity I, a well-defined potential $V_g = I \cdot R$ is imposed between the grid and the grounded plate on which the samples are placed.

Part of the charge generated by the corona electrode will be discharged to ground through the resistors connected to the grid, the other part, the ions which pass through the grid, will be retained by the surface of the sample. The potential at the surface of the sample is limited by the potential of the grid V_g or by the partial discharges of the deposited charge.

In all the experiments described hereafter, the samples were charged for 10 s. The grid potential V_g = 1.2 kV for negative and positive polarity.

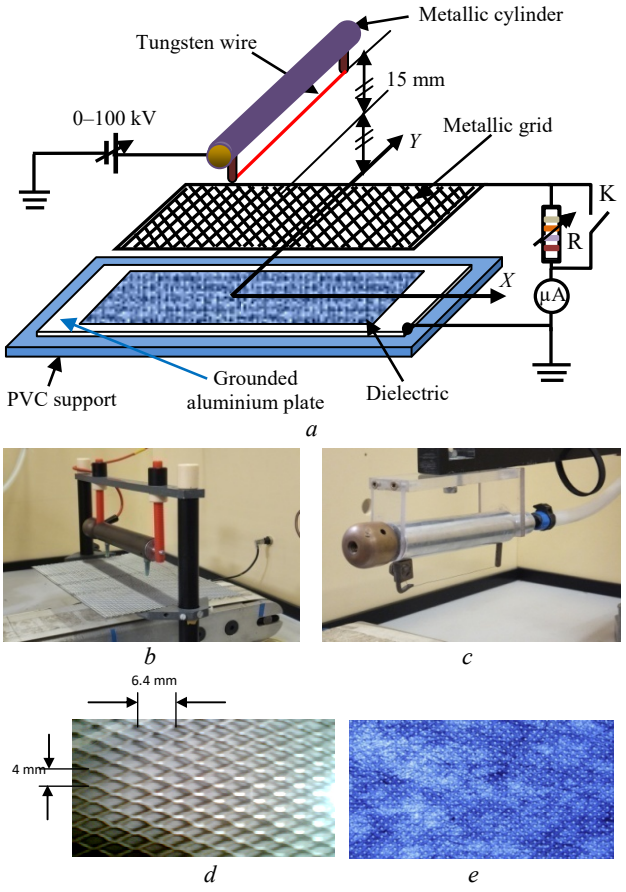

Fig. 1. *a* – configuration of electrode system type «triode» used for charging and neutralization; *b* – triode system «wire – grid – plane»; *c* – dual electrode system used for neutralization; *d* – metallic grid; *e* – fibrous polypropylene sample

The sample carrier consisted of a polyvinyl chloride PVC plate; to which plate electrode was firmly fixed. A conveyor belt supported the sample carrier and transferred it from the charging position to the surface potential measurement and charge neutralization sections of the experimental set-up. The speed of the conveyor can be adjusted from 1 cm/s to 6 cm/s, for the various needs of the experiments.

The efficiency of the neutralization is obtained by comparing the profiles of the potential of the surface charge before and after neutralization [8, 24]. Non-contact measurement of the surface potential is used to take multiple profiles without affecting the sample charge state.

As soon as the HV supply of the corona charger was turned off, the conveyor belt transferred the samples at a constant speed through the measurement section. Thus the repartition of the surface potential along the central axis OX of the sample was measured with an electrostatic voltmeter (model 341B), equipped with an electrostatic probe (model 3450, Trek Inc., Medina, NY), and recorded via an electrometer (model 6514, Keithley Instruments, Cleveland), connected to a computer. The acquisition and processing of experimental data was performed using an ad-hoc virtual instrument, developed in LabView environment.

In the first part of the experiment the neutralization was performed with a dual wire-type electrode similar to the one described above. The neutralizer–sample spacing was 50 mm (Fig. 2).

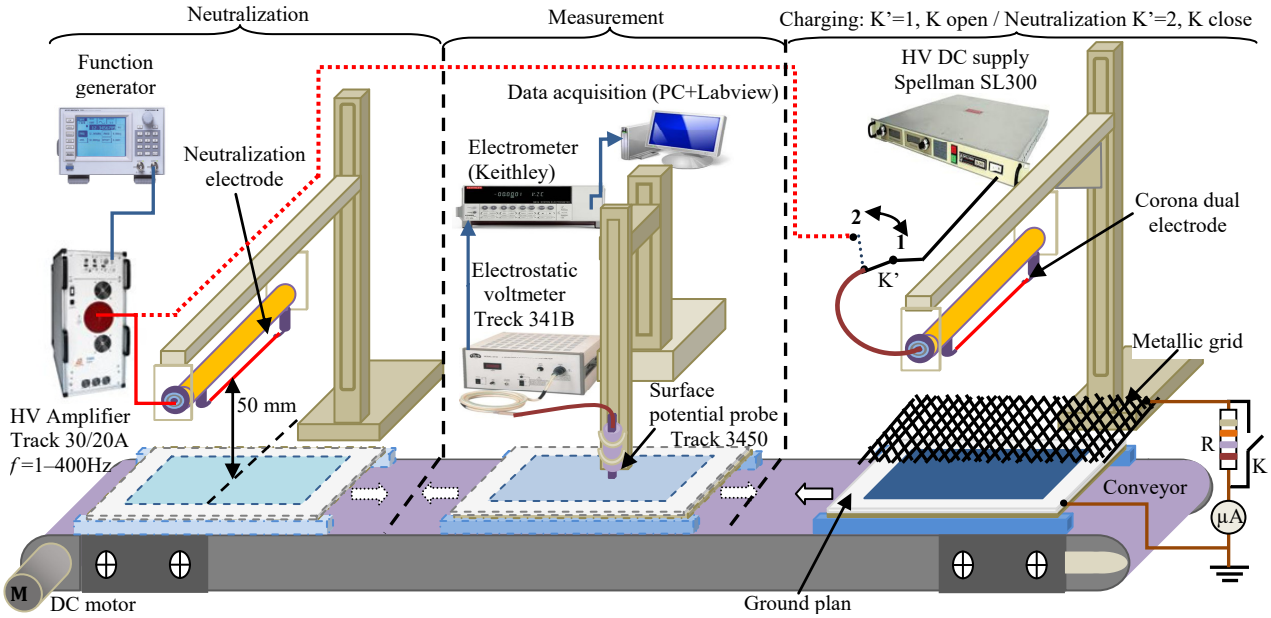

Fig.2. Experimental setup

In the second part of the experiment, the neutralization is carried out by the triode system, used previously to charge the sample, by closing the switch *K* and putting the switch K' on position 2 (Fig. 2). Closing the switch K imposes a zero potential to the grid. The intensity of the discharge is measured by the micro-ammeter connecting the grid to the ground. In both systems, the neutralization electrode was connected to a HV amplifier 30 kV, 20 mA (model 30/20A, Trek Inc., Medina, NY).

The amplitude U_n and the frequency f of the HV were adjusted using a synthesized function generator (model FG300, Yokogawa, Japan). In order to follow the decay of the surface potential and get a relatively stable charge, neutralization is carried out after 300 s of the charging turn off. For both neutralizing electrode configurations, the corona electrode is energized by high alternative voltage at industrial frequency (50 Hz).

The neutralization with the dual electrode system is performed in motion at a speed of 3 cm/s.

In triode configuration, the neutralization is in static mode, the sample is centered under the active electrode of the triode system during the discharge which takes 4 s. The profiles of the surface potential are obtained just before and after the neutralization using the previously described method.

Each experiment was repeated 3 times, and each run is performed on a new sample. If the tests show a disparity, further tests will be performed.

The neutralization rate N % is expressed as a function of V_{01} and V_{02}, the maximum recorded values (absolute values) of the potential along the central axis OX of the sample, respectively before and after neutralization:

$$N\,[\%] = [1 - \text{abs}\,(V_{02}/V_{01})]\cdot 100. \qquad (1)$$

In the first part of the experiments, we used the dual system, the amplitude of the sinusoidal neutralization voltage was varied through 6 levels: U_n = 16, 18, 20, 21, 22, 24 kV at 50 Hz frequency. In the second part of the experiments, the neutralization is carried out by 3 sinusoidal voltage amplitudes: U_n = 6, 12.5, 15 kV, associated with respectively 3 grid current values: I_g = 10, 50, 100 μA.

Results and discussion. The non-uniform distribution of the surface potential is due to the inhomogeneous structure of the non-woven dielectric and the partial discharges that can occur due to the local intensification of the electric field [26, 27].

Samples are charged for 10 s with positive or negative corona discharge. Each test is carried out on a new sample. The neutralization is performed after 300 s after charging, so that any variations in the profile of the surface potential before and after neutralization are only linked to the neutralization and not to the decline [6]. Thus, the effect of the surface potential decay on the efficiency of neutralization can be neglected. The decay of surface potential is due to the combined action of several physical mechanisms (partial discharges, recombination, lateral and transversal conduction) and also influenced by the value of the charge potential [6, 26, 27].

The efficiency of the neutralization of electrostatic charges on the surface of the dielectric is obtained by comparing the surface potential profiles just before and after neutralization. It is calculated as the ratio between the maximum electrical potential measured at the surface of the dielectric before (V_{01}) and after exposing them to the bipolar ions generated by an AC corona discharge (V_{02}) [23, 24].

Dual electrode system neutralization efficiency. In the neutralization with the dual system, the sample passes through the AC zone discharge with a constant speed of 3 cm/s. Several amplitude values of the corona electrode voltage were tested.

Figures 3, 4 show the surface potential profiles before and after neutralization with a double electrode system at high sinusoidal voltages at the frequency of 50 Hz. We notice a non-symmetry of the surface potential profiles shown in these figures and this is due to the inhomogeneous surfaces and structures of the samples used (non-woven fabric). Symmetry will be obtained if the samples are with a homogeneous surface such as films are used.

At the amplitude of 16 kV, the neutralization did not occur; this is due to the fact that this amplitude value is slightly higher than the threshold value of the corona

discharge. The few electrons created in the ionization zone do not have enough energy to ionize other molecules and create other additional electrons. The positive ions do not have time to leave the drift zone before the arrival of the negative alternation (Fig. 3,*a*). On the other hand, for the positive charge, we notice a significant neutralization where the maximum potential is 1.29 kV and decreases to 0.81 kV after neutralization. This means that the negative ions arrive at the surface of the sample before the positive half-wave, due to the fact, that the mobility of the negative ions is greater than that of the positive ions as shown in Fig. 4,*a*.

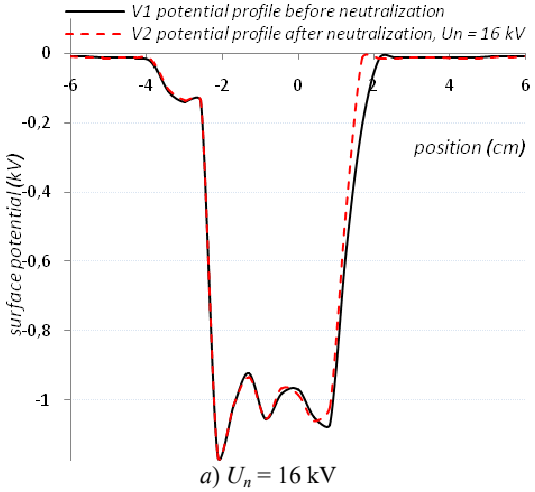

a) U_n = 16 kV

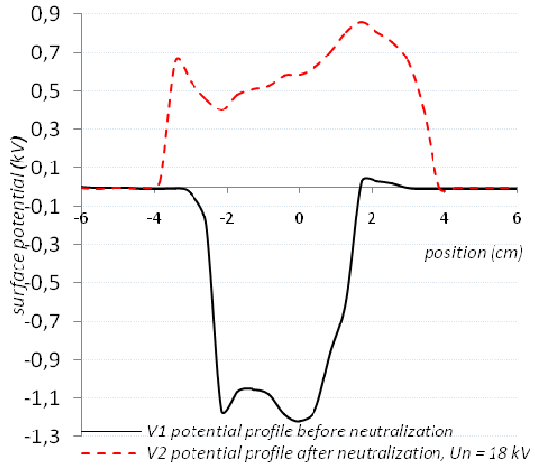

b) U_n = 18 kV

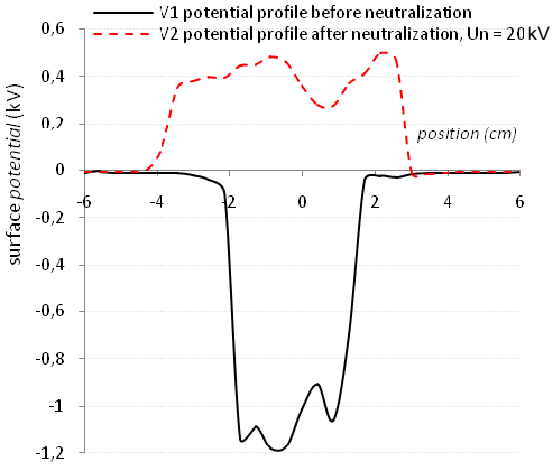

c) U_n = 20 kV

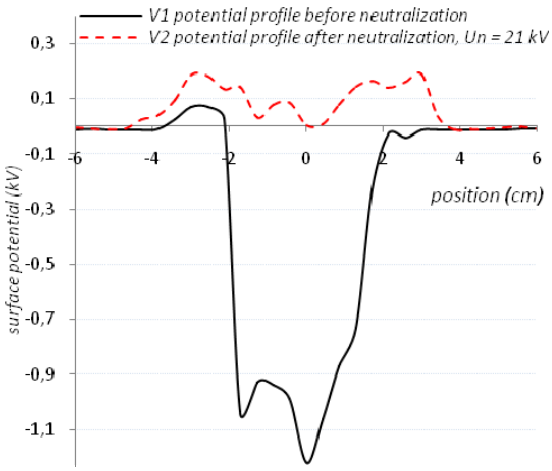

d) U_n = 21 kV

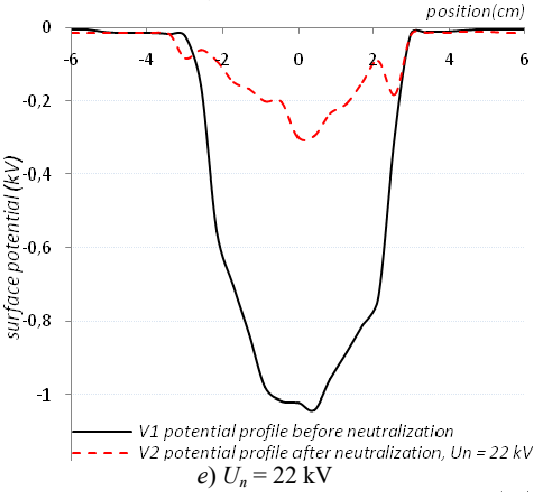

e) U_n = 22 kV

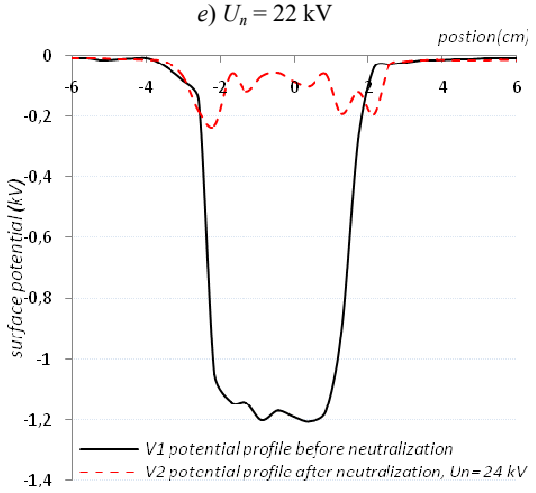

f) U_n = 24 kV

Fig. 3. Typical surface potential profiles before and after neutralization with dual electrode, <u>*negative*</u> initial charge

At the large inter-electrode distances or at weak electric fields, there is an accumulation of space charges. Indeed; for weak electric fields the positive ions do not have time to be evacuated during the positive alternation. Their presence around the conductor increases the existing electric field. Therefore the following discharge mode takes place at a lower applied voltage.

However, in the neutralization with a voltage of 18 kV, the potential after neutralization is positive, with 856 V as the maximum value, while the initial potential was negative with a maximum value of |–1.2| kV. This means that all the initial charges are completely neutralized and new charges

are deposited (Fig. 3,*b*). The surface occupied by the positive charges is wider than the initial negatively charged surface; this difference is due to the mode of charge and neutralization; fixed mode for depositing the charge and scanning mode for neutralization. For the initial positive charge, the neutralization is greater but the polarity of the charge on the sample has not changed. The maximum potential decreases from 1010 V to 231 V after neutralization (Fig. 4,*b*).

Figures 3,*c*,*d* illustrate the profiles of the surface potential before and after neutralization with the amplitudes of sinusoidal high voltages of 20 kV and 21 kV respectively. The initial negative charges are completely neutralized and positive charges are deposited at the surface of samples.

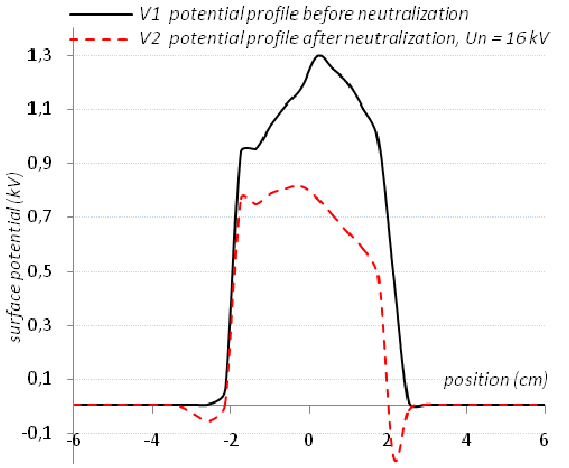

a) U_n = 16 kV

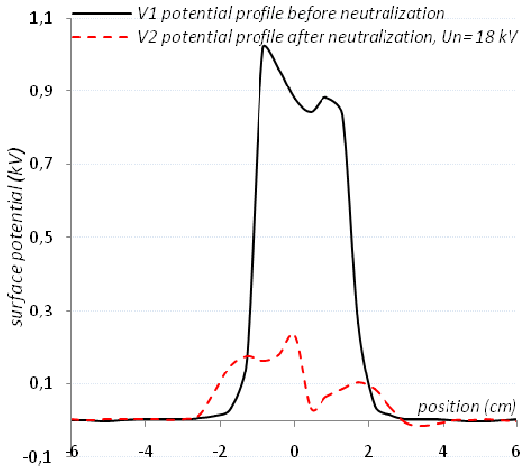

b) U_n = 18 kV

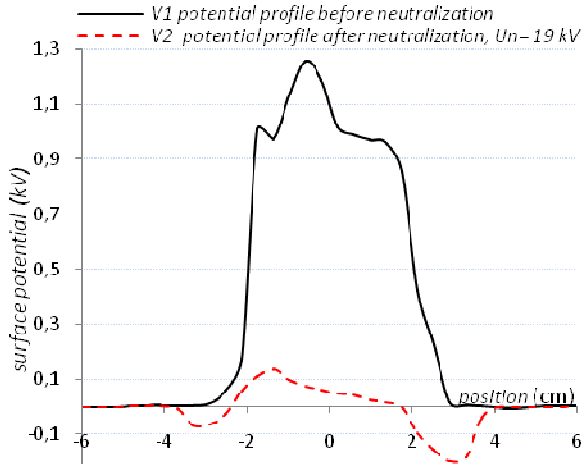

c) U_n = 19 kV

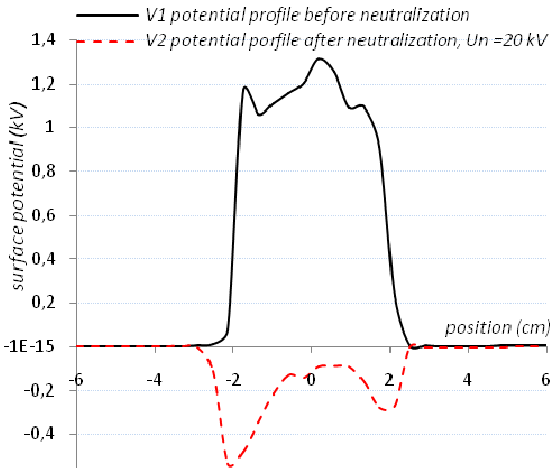

d) U_n = 20 kV

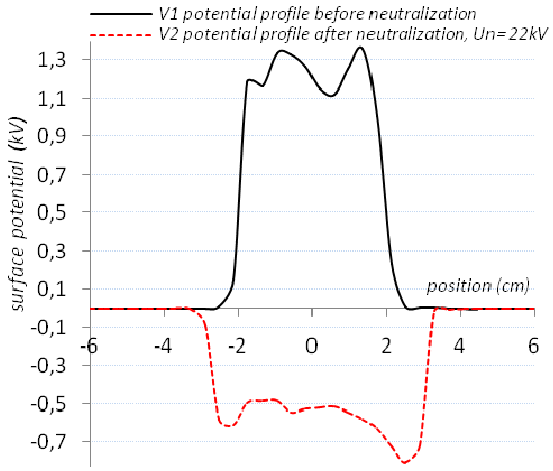

e) U_n = 22 kV

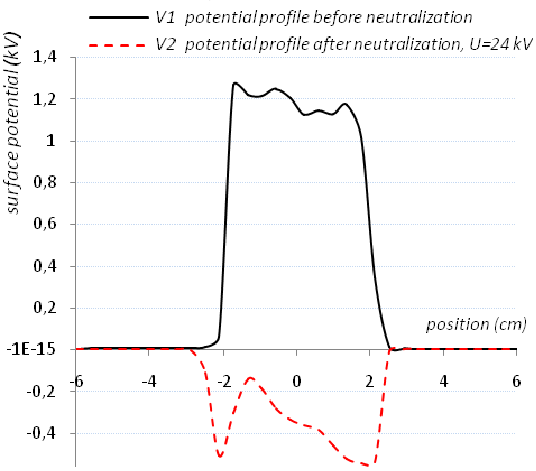

f) U_n = 24 kV

Fig. 4. Typical surface potential profiles before and after neutralization with dual electrode, *positive* initial charge

The charge deposited by the magnitude of 20 kV is greater than that registered by the amplitude of 21 kV. The maximum values of the surface potential after neutralization are 500 V and almost 200 V for the amplitudes 20 kV and 21 kV respectively. At these voltage amplitude values, the electric field is not strong enough to create a significant number of positive ions and allow them to reach the sample surface during the positive half-wave. While for the initial positive charge, this is completely neutralized and there is a deposit of new negative charge as shown in Fig. 4,*c*,*d*. This means that the positive charge on

the surface of the samples contributed to the corona discharge by reinforcing the electric field during the negative half-wave and reducing it during the positive half-wave. Knowing that, the negative corona discharge appears at higher voltages than the positive corona discharge.

However, at the amplitudes of 22 and 24 kV, the surface potential is negative after neutralization with maximum values |–230| V and |–300| V respectively (Fig. 3,*e*,*f*). These results show the existence of a value of voltage between 21 kV and 22 kV which provides complete neutralization without depositing new charges.

For the initial positive charges, after neutralization we have deposition of new negative charges, where the maximum surface potentials are |–809| V and |–538| V for the respective amplitudes of 22 kV and 24 kV (Fig. 4,*e*,*f*). This means that all the initial charge is completely neutralized.

At the alternating voltage amplitudes greater than 22 kV, the positive ions produced during the positive half-wave do not all have time to be evacuated before the arrival of the negative half-wave. This positive space charge reinforces the electric field during the negative alternation and the majority of the ions which arrive at the surface of the sample are negative ions. In this case, there will be a tendency to deposit a negative charge on the surface of the samples.

The variation of the neutralization rate N [%] and the ratio V_{02}/V_{01} [%] are displayed in Fig. 5. V_{01} and V_{02} are respectively the maximum values of the surface potential before and after neutralization. When the samples are negatively charged, at the voltage of 16 kV, the potentials V_{01} and V_{02} are too close; with this amplitude no neutralization is obtained. However, for the voltages of 18, 20, 21 kV, the surface potential after neutralization is positive whereas the potential before neutralization was negative.

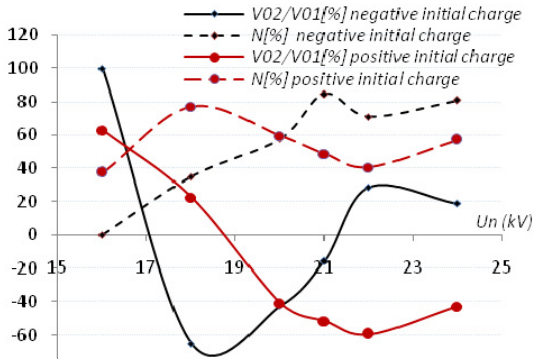

Fig. 5. Surface potential ratio V_{02}/V_{01} [%] and neutralization rate N [%] as a function of high sinusoidal voltage amplitudes U_n (kV) for 2 polarities of deposited charges

The change of sign of the rate V_{02}/V_{01} means that the initial charge is completely neutralized and a new charge of opposite sign is deposited. This also means that complete neutralization and without deposition of any new charge can be achieved in this voltage range.

The maximum neutralization of a rate greater than 85 % is obtained at the voltage of 21 kV. On the other hand, when the samples are positively charged, at a voltage of 16 kV, we obtain a neutralization rate of almost 38 % and the maximum neutralization of almost 78 % at 18 kV. This means that at these voltages, the charge on the sample contributes to the discharge. However, for voltages of 20, 21, 22, 24 kV, the surface potential after neutralization is negative while the potential before neutralization was positive.

The change in sign of the voltage ratio V_{02}/V_{01} means that complete neutralization and without deposition of new charge can be achieved in the range of voltage.

We note for the voltages of 22 kV and 24 kV the charge on the surface of the samples is negative whatever the initial charge of the samples.

Neutralization efficiency of the triode system. Samples are charged for 10 s by negative corona discharge with current intensity I = 50 μA. The neutralization is carried out with triode system in static mode. The corona electrode of the triode system of neutralization is powered by alternating sinusoidal voltages corresponding 6, 12.5 and 15 kV with associated grid currents intensity I_g of 10, 50 and 100 μA respectively. The samples are exposed for 4 s to bipolar ions generated by an alternating corona discharge (AC).

Figure 6 shows the surface potential profiles before and after neutralization with high alternating voltages, for 3 HV sinusoidal amplitude (6, 12.5 and 15 kV). The profile of the surface potential is slightly affected at the extremities of the potential profile, where there was a decrease of a few volts due to exposure to the corona discharge at the amplitude of 6 kV associated to the current grid of 10 μA (Fig. 6,*a*). At this amplitude, there is not any neutralization obtained in the middle of the sample. This means that the discharge intensity is not sufficient and most of the ions lose their charges by hitting the grid connected to ground [30].

The discharge is between the active electrode and the grid. However, the amplitude voltage of 12.5 kV, associated to grid current intensity I_g = 50 μA, a maximum neutralization is achieved in the middle of the sample, just below the corona electrode, with a surface potential close to –25 V.

At the edges of the profile, the surface potential is similar to the profile before naturalization, this means that the energy of the discharge is not sufficient to allow the neutralizing charges to deflect towards the sample extremities (Fig. 6,*b*) [20, 25].

The surface potential profiles obtained before and after neutralization with the voltage amplitude of 15 kV, associated to grid current of 100 μA are presented in Fig. 6,*c*.

At this voltage, almost all the deposited charges are neutralized. The surface potential profile after neutralization is completely flattened with a small peak surface potential with a value that does not exceed –40 V. Indeed, under these conditions the corona discharge is assisted by an intense electric field which accelerates a portion of the positive ions and allows them to reach the negatively charged surface of the sample [28].

So, the neutralization of electrostatic charges on the surface of a fibrous dielectric material is more efficient at higher voltage and higher current intensities of alternative corona discharge.

Figure 7 presents the variation of the neutralization rate N [%] and the ratio V_{02}/V_{01} [%] as function of the neutralization voltage with the triode system, V_{01} and V_{02} being respectively the maximum values of the surface potential before and after neutralization. At the amplitude of 6 kV, the neutralization is not obtained, the surface

potential profiles before and after neutralization are almost the same ($V_2 \approx V_1$). However, for the amplitude of 12.5 kV, the ratio of surface potentials just before and after neutralization V_{02}/V_{01} is equal to 40 %, which leads to a neutralization rate of 60 %.

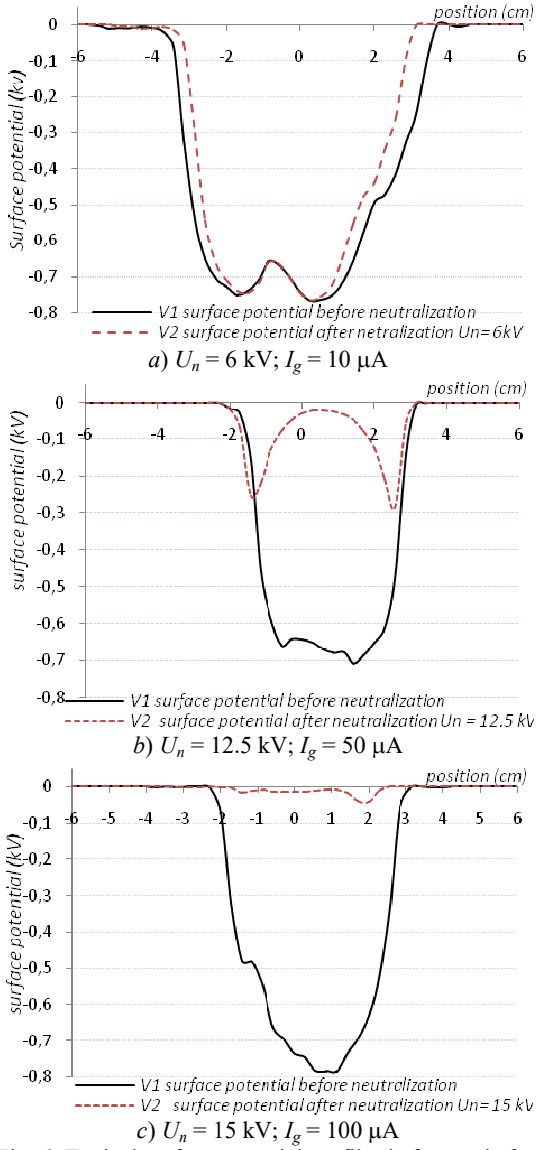

a) U_n = 6 kV; I_g = 10 μA

b) U_n = 12.5 kV; I_g = 50 μA

c) U_n = 15 kV; I_g = 100 μA

Fig. 6. Typical surface potential profiles before and after neutralization with triode electrode system

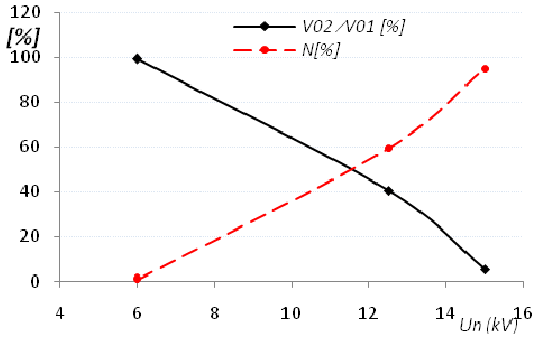

Fig. 7. Neutralization rate N [%] and surface potential ration V_{02}/V_{01} [%] as function of the neutralization voltage U_n, kV

For the neutralization voltage of amplitude 15 kV, an almost complete neutralization of 95 % of the charges deposited on the sample surface is achieved. The results show that the ratio V_{02}/V_{01} is positive for all voltage level; this means that there is no deposition of a new charge of the same polarity or of polarity opposite to the initial charge.

Indeed, with the neutralization by triode system, only ions of polarity opposite to the charges of the dielectric can cross the grid, due to the fact that the electric field is reinforced by the negative surface charge of the sample during the positive alternation.

However, the field is weakened by the negative charges on the sample surface during the negative alternation. The negative ions will therefore be repelled by the negative charges of the sample and evacuated from the grid towards the ground. During the negative alternation, the discharge is between the corona electrode and the grid.

Conclusions. The neutralization by high alternating voltages at industrial frequency is an advantage; this allows the network voltage to be used by amplifying only the voltage without any frequency adjustment.

Dual system. For certain voltages levels, the entire initial charge is neutralized but new charges of opposite sign are deposited. Proper adjustment of the exposure time and amplitude of the high voltage is necessary to ensure neutralization of all charges without depositing new ones. For low neutralization voltage amplitudes, the polarity of the charge to be neutralized has a significant effect on the neutralization rate.

Triode system. The neutralization with the triode system is more efficient, the grid connected to the ground prevents the deposition of new charges of opposite sign on the surface of the fibrous media. There is no deposition of new charge. The neutralization efficiency of electrostatic charge is proportional to the intensity of the discharge current. It is important to find the relationship between the exposure time and the intensity of the discharge with the neutralization efficiency. In industrial applications, the neutralization in scan mode is more convenient. The efficiency of the neutralization using a triode system can be improved by scan mode and optimizing its scanning speed.

Conflict of interest. The authors declare that they have no conflicts of interest.

REFERENCES

1. Young R.H. Kinetics of xerographic discharge by surface charge injection. *Journal of Applied Physics*, 1992, vol. 72, no. 7, pp. 2993-3004. doi: https://doi.org/10.1063/1.351507.

2. Zhou Q., Li L., Bi X., Zhang G., Cao Z., Meng H., Lan Q., Liang C., Chen X., Ma J. Electrostatic elimination of charged particles by DC-type bipolar electrostatic eliminator. *Powder Technology*, 2022, vol. 408, art. no. 117774. doi: https://doi.org/10.1016/j.powtec.2022.117774.

3. Benaouda I., Zelmat M.E.M., Ouiddir R., Dascalescu L., Tilmatine A. Analysis of a novel insulating conveyor-belt tribo-electrostatic separator for highly humid granular products. *Journal of Electrostatics*, 2019, vol. 100, art. no. 103357. doi: https://doi.org/10.1016/j.elstat.2019.103357.

4. Kang M.S., Yu G., Shin J., Hwang J. Collection and decomposition of oil mist via corona discharge and surface dielectric barrier discharge. *Journal of Hazardous Materials*, 2021, vol. 411, art. no. 125038. doi: https://doi.org/10.1016/j.jhazmat.2021.125038.

5. Kachi M., Nemamcha M., Lazhar H., Dascalescu L. Neutralization of charged insulating granular materials using AC corona discharge. *Journal of Electrostatics*, 2011, vol. 69, no. 4, pp. 296-301. doi: https://doi.org/10.1016/j.elstat.2011.04.005.

6. Tabti B., Yahiaoui B., Bendahmane B., Dascalescu L. Surface potential decay dynamic characteristics of negative-corona-charged fibrous dielectric materials. *IEEE Transactions on Dielectrics and Electrical Insulation*, 2014, vol. 21, no. 2, pp. 829-835. doi: https://doi.org/10.1109/TDEI.2013.003854.

7. Antoniu A., Tabti B., Plopeanu M.-C., Dascalescu L. Accelerated Discharge of Corona-Charged Nonwoven Fabrics. *IEEE Transactions on Industry Applications*, 2010, vol. 46, no. 3, pp. 1188-1193. doi: https://doi.org/10.1109/TIA.2010.2045331.
8. Yahiaoui B., Tabti B., Megherbi M., Antoniu A., Plopeanu M.-C., Dascalescu L. AC corona neutralization of positively and negatively charged polypropylene non-woven fabrics. *IEEE Transactions on Dielectrics and Electrical Insulation*, 2013, vol. 20, no. 5, pp. 1516-1522. doi: https://doi.org/10.1109/TDEI.2013.6633678.
9. Moreau E., Benard N. Ionic wind produced by volume corona discharges and surface dielectric barrier discharges: What role do streamers play? *Journal of Electrostatics*, 2024, vol. 132, art. no. 103988. doi: https://doi.org/10.1016/j.elstat.2024.103988.
10. Boiko M.I., Makogon A.V. Features of distribution of electric field strength and current density in the reactor during treatment of liquid media with high-voltage pulse discharges. *Electrical Engineering & Electromechanics*, 2024, no. 5, pp. 58-63. doi: https://doi.org/10.20998/2074-272X.2024.5.08.
11. Molchanov O., Krpec K., Horák J. Nox removal from Small-Scale biomass combustion in DC Corona: Influence of discharge polarity on plasma chemical kinetics. *Chemical Engineering Science*, 2024, vol. 300, art. no. 120597. doi: https://doi.org/10.1016/j.ces.2024.120597.
12. Huang H., Chen W., Mi J., Zhang Y., Bi N., Du S. Study on the application of atomized corona discharge combined with screen electrode in dust collection. *Journal of Electrostatics*, 2024, vol. 130, art. no. 103953. doi: https://doi.org/10.1016/j.elstat.2024.103953.
13. Hassan W., Shafiq M., Hussain G.A., Choudhary M., Palu I. Investigating the progression of insulation degradation in power cable based on partial discharge measurements. *Electric Power Systems Research*, 2023, vol. 221, art. no. 109452. doi: https://doi.org/10.1016/j.epsr.2023.109452.
14. Tuan Dung N., Besse C., Rogier F. An implicit time integration approach for simulation of corona discharges. *Computer Physics Communications*, 2024, vol. 294, art. no. 108906. doi: https://doi.org/10.1016/j.cpc.2023.108906.
15. Tao S., Zhu Y., Chen C., Liu J., Chen M., Shangguan W. Removal of air pollutant by a spike-tubular electrostatic device: Multi-stage direct current corona discharge enhanced electrostatic precipitation and oxidation ability. *Process Safety and Environmental Protection*, 2022, vol. 165, pp. 347-356. doi: https://doi.org/10.1016/j.psep.2022.06.069.
16. Abouelatta M.A., Ward S.A., Sayed A.M., Mahmoud K., Lehtonen M., Darwish M.M.F. Measurement and assessment of corona current density for HVDC bundle conductors by FDM integrated with full multigrid technique. *Electric Power Systems Research*, 2021, vol. 199, art. no. 107370. doi: https://doi.org/10.1016/j.epsr.2021.107370.
17. Khalifehei M., Higuera F.J. Neutralization of an electrospray by a corona discharge. *Journal of Aerosol Science*, 2020, vol. 145, art. no. 105547. doi: https://doi.org/10.1016/j.jaerosci.2020.105547.
18. Mustika W.S., Hapidin D.A., Saputra C., Munir M.M. Dual needle corona discharge to generate stable bipolar ion for neutralizing electrosprayed nanoparticles. *Advanced Powder Technology*, 2021, vol. 32, no. 1, pp. 166-174. doi: https://doi.org/10.1016/j.apt.2020.11.026.
19. Oudaifia N., Kachi M., Moussaoui A., Boudefel A. Cylindrical electrodes for neutralization of insulating flowing particles. *Journal of Electrostatics*, 2021, vol. 110, art. no. 103556. doi: https://doi.org/10.1016/j.elstat.2021.103556.
20. Settaf B., Ziari Z., Sahli S. Effect of the applied high voltage on the neutralization efficiency of negative charges accumulated on polypropylene film surface. *2023 International Conference on Electrical Engineering and Advanced Technology (ICEEAT)*, 2023, pp. 1-4. doi: https://doi.org/10.1109/ICEEAT60471.2023.10426438.
21. Messaoudène A., Mekidèche M.R., Bendahmane B., Tabti B., Dascalescu L. Experimental study of controlled active neutralization of polypropylene films. *Journal of Electrostatics*, 2020, vol. 103, art. no. 103407. doi: https://doi.org/10.1016/j.elstat.2019.103407.
22. Messaoudene A., Mekideche M.R., Bendahmane B., Tabti B., Medles K., Dascalescu L. Optimization of the Active Neutralization of Polypropylene Film Using Response Surface Methodology. *IEEE Transactions on Industry Applications*, 2020, vol. 56, no. 5, pp. 5463-5471. doi: https://doi.org/10.1109/TIA.2020.3001538.
23. Yahiaoui B., Megherbi M., Smaili A., Antoniu A., Tabti B., Dascalescu L. Distribution of Electric Potential at the Surface of Corona-Charged Polypropylene Nonwoven Fabrics After Neutralization. *IEEE Transactions on Industry Applications*, 2013, vol. 49, no. 4, pp. 1758-1766. doi: https://doi.org/10.1109/TIA.2013.2256412.
24. Yahiaoui B., Megherbi M., Tabti B., Dascalescu L. Sinusoidal, Triangular, or Square Alternating Voltages Neutralization of Electrostatic Charges on the Surface of Polypropylene Nonwoven Fabric. *IEEE Transactions on Industry Applications*, 2015, vol. 51, no. 1, pp. 685-691. doi: https://doi.org/10.1109/TIA.2014.2336985.
25. Bendahmane B., Messaoudene A., Dascalescu L. Alternating Current Corona neutralization of charged filters media. *2020 IEEE 3rd International Conference on Dielectrics (ICD)*, 2020, pp. 910-913. doi: https://doi.org/10.1109/ICD46958.2020.9341941.
26. Chen G. A new model for surface potential decay of corona-charged polymers. *Journal of Physics D: Applied Physics*, 2010, vol. 43, no. 5, art. no. 055405. doi: https://doi.org/10.1088/0022-3727/43/5/055405.
27. Malathip K., Techaumnat B., Sasamoto R., Nishijima K. Experimental and Numerical Study on the Charge Decay on Solid Insulator Surface. *2020 8th International Conference on Condition Monitoring and Diagnosis (CMD)*, 2020, pp. 430-433. doi: https://doi.org/10.1109/CMD48350.2020.9287267.
28. Messaoudene A., Mekideche M.R., Bendahmane B., Tabti B., Medles K., Dascalescu L. Experimental modeling and optimization of the active neutralization of a PP film, using design of experiments methodology. *2019 IEEE Industry Applications Society Annual Meeting*, 2019, pp. 1-4. doi: https://doi.org/10.1109/IAS.2019.8912025.
29. Messaoudène A., Dascalescu L., Bendahmane B., Yahiaoui B., Mekidèche M. R. Experimental study of the active and controlled neutralization of polypropylene nonwoven media. *Electrical Engineering International Conference (EEIC'2019)*, 4-5 December 2019, Bejaia, Algeria.
30. Bouteffaha A., Bendaoud A., Reguig A., Dascalescu L. Effects of the grid geometry on the performances of a triode-type corona electrode system. *Journal of Electrostatics*, 2019, vol. 101, art. no. 103367. doi: https://doi.org/10.1016/j.elstat.2019.103367.

Received 04.11.2024
Accepted 31.01.2025
Published 02.05.2025

B. Yahiaoui[1], *PhD, Lecturer,*
A. Messaoudene[1], *PhD, Lecturer,*
A. Melahi[1], *PhD Student, Lecturer,*
A. Rahmani[1], *PhD, Lecturer,*
B. Bendahmane[1], *PhD, Professor,*
L. Dascalescu[2], *PhD, Professor,*
[1] Electrical Engineering Department,
University of Bejaia, Algeria,
e-mail: belkacem.yahiaoui@univ-bejaia.dz (Corresponding Author)
[2] Université de Poitiers, France.

How to cite this article:
Yahiaoui B., Messaoudene A., Melahi A., Rahmani A., Bendahmane B., Dascalescu L. Efficiency of neutralization of electric charges on the surface of dielectric nonwoven fabric of two dual and triode electrode systems. *Electrical Engineering & Electromechanics*, 2025, no. 3, pp. 76-83. doi: https://doi.org/10.20998/2074-272X.2025.3.11